Xu *et al. Surface Science and Technology* (2023) 1:5
https://doi.org/10.1007/s44251-023-00004-7

Surface Science and Technology

ORIGINAL ARTICLE Open Access

Adsorption and surface reactions of C_2H_2 and C_2H_4 on Co(0001)

Lingshun Xu[1,2], Zongfang Wu[1], Haocheng Wang[1], Junjie Shi[1], Zichen Li[1] and Weixin Huang[1*]

Abstract

In this paper we have studied adsorption and surface reactions of acetylene and ethylene on Co(0001) in detail by temperature desorption spectrum (TDS), X-ray photoelectron spectroscopy (XPS) and ultraviolet photoelectron spectroscopy (UPS). C_2H_4 adsorption at 130 and 300 K followed by subsequent heating mainly forms C_2 clusters and graphitic carbon, respectively, while C_2H_4 decomposes at 400 and 500 K to form dominant graphitic carbon and carbon adatoms, respectively. C_2H_2 molecularly adsorbs at 130 K but exclusively dehydrogenates upon heating. The resulting C_2H_2(a) species at low coverages remains stable up to 400 K and then exclusively dehydrogenates into C_2 clusters, while the resulting C_2H_2(a) species at high coverages remains stable up to 310 K and then majorly dehydrocyclizates into $(C_2H)_n$ intermediates with ring structures at 340 K which further dehydrogenates into graphitic carbon, and minorly dehydrogenates into C_2 clusters. Exposed at 370 K, C_2H_2 dehydrocyclizates into $(C_2H)_n$ intermediates with ring structures. These temperature and coverage dependent surface reactions of C_2H_2 and C_2H_4 on Co(0001) greatly enrich our fundamental understanding of Co-catalyzed F-T synthesis reaction.

Keywords Surface chemistry, Fischer–Tropsch synthesis, Graphene growth, Cobalt, Reaction mechanism

1 Introduction

Heterogeneous catalytic reactions usually involve complex surface reaction networks on solid catalysts, whose fundamental understanding has been mostly achieved by studying model catalysts with well-defined surface structures and surface species under well-controlled conditions [1–3]. The Fischer–Tropsch synthesis (FTS) is an important catalytic reaction transforming the syngas ($CO+H_2$) into higher hydrocarbons, such as gasoline, diesel, and kerosene [4–12]. Cobalt catalysts exhibit low temperature, high activity, high chain growth probability, and high stability in the FTS process [13] This has motivated many fundamental studies of adsorption, surface reactions and desorption of reactants (CO and H_2), products (hydrocarbons and H_2O) and intermediates (carbon species, oxygen species, CH_x and C_xH_y) experimentally on Co single crystal model catalysts and polycrystalline Co [14–34] and theoretically using density functional theory (DFT) calculations [35–42].

Acetylene and ethylene are among the major products of FTS. C_2H_4 was reported to dehydrogenate on polycrystalline cobalt at room temperature into acetylene which partially dissociated into CH-like species at elevated temperatures [30] but to completely decomposed on Co(0001) into C and H adatoms via acetylene intermediate below room temperature [31]. Later studies found that adsorption and surface reactions of C_2H_4 on Co(0001) depended on the available vacant surface sites, leading to formation of carbon adatoms, C_2 clusters and graphitic carbon [18, 21]. Adsorption and surface reactions of C_2H_2 on Co single crystals were also studied [31–34]. Varri et al. [32] reported that C_2H_2 molecularly adsorbed on Co(0001) at room temperature and

*Correspondence:
Weixin Huang
huangwx@ustc.edu.cn
[1] Key Laboratory of Precision and Intelligent Chemistry, Hefei National Research Center for Physical Sciences at the Microscale, iChEM, Key Laboratory of Surface and Interface Chemistry and Energy Catalysis of Anhui Higher Education Institutes, Department of Chemical Physics, University of Science and Technology of China, Hefei 230026, P.R. China
[2] Anhui Huishu Iot Technology Co., LTD, Hefei 230601, P.R. China

Springer

decomposed to form a likely vinylidene (CCH_2) intermediate at 410 K and eventually graphitic and carbidic carbon species at elevated temperatures, whereas Ramsvik et al. [33, 34] proposed CH or C_2 fragments as surface intermediates of C_2H_2 decomposition on Co(0001) and (11–20) surfaces. Thus, arguments exist on adsorption and surface reactions of C_2H_4 and C_2H_2 on Co surfaces. In this paper we used temperature desorption spectrum (TDS), X-ray photoelectron spectroscopy (XPS) and ultraviolet photoelectron spectroscopy (UPS) to study adsorption and surface reactions of acetylene and ethylene on Co(0001) and observed temperature and coverage dependent surface reactions of C_2H_2 and C_2H_4 on Co(0001).

2 Methods

All experiments were performed in a Leybold stainless-steel ultrahigh vacuum (UHV) chamber with a base pressure of 1.2×10^{-10} mbar [17] The UHV chamber was equipped with facilities for XPS, UPS, LEED, and differential-pumped TDS measurements, in which new hemispherical energy analyzer (PHBIOS 100 MCD, SPECS GmbH), x-ray source (XR 50, SPECS GmbH) and UV source (UVS 10/35, SPECS GmbH) were recently installed. A Co(0001) single crystal purchased from MaTeck was mounted on the sample holder by two Ta wires spot-welded to the back side of the sample. The sample temperature could be controlled between 120 and 1473 K and was measured by a chromel–alumel thermocouple spot-welded to the back side of the sample. Prior to the experiments, the Co(0001) sample was cleaned by repeated cycles of Ar ion sputtering and annealing until LEED gave a sharp (1 × 1) diffraction pattern and no contaminants could be detected by XPS. The annealing temperature of Co(0001) was kept always below 650 K to avoid the likely transition of from hcp Co(0001) to fcc structure.

C_2H_4 (> 99.9999%, Arkonic Gases & Chemicals Inc.), C_2H_2 (> 99.99%, Nanjing ShangYuan Industry Factory), O_2 (> 99.99%, Nanjing ShangYuan Industry Factory), and H_2 (> 99.999%, Nanjing ShangYuan Industry Factory) were used as received and their purity was further checked by quadrupole mass spectrometer (QMS) prior to experiments. The base pressure of the chamber during the course of C_2H_4 and C_2H_2 exposure was controlled to be below 5×10^{-10} torr, therefore, a line-of-sight stainless steel doser (diameter: 8 mm) positioned ~ 2 mm in front of the Co(0001) surface was used for relatively large C_2H_4 and C_2H_2 exposures. The doser could be retracted 50 mm after the exposure. The enhancement factor of the doser was calibrated to be 920 by comparing the H_2O desorption peak areas of H_2O TDS spectra followed exposures of 0.005 L H_2O at 130 K by back filling and by the doser [17]. The exposures of C_2H_4 reported herein were corrected with the enhancement effect of the doser. Other gases were dosed by back filling. All exposures were reported in Langmuir (1 L = 1.0×10^{-6} Torr s) without corrections for the gauge sensitivity.

During the TDS experiments, the Co(0001) surface was positioned ~ 1 mm away from the collecting tube of a differential-pumped QMS and heated to 630 K with a heating rate of 3 K/s. The signals with m/e = 2 (H_2), 18 (H_2O), 25 (C_2H_2 and C_2H_4), 26 (C_2H_2 and C_2H_4), 27 (C_2H_4), 28 (C_2H_4 and CO), 30 (C_2H_6), and 44 (CO_2) were monitored. XPS spectra were recorded using Al K_α radiation (hν = 1486.6 eV) with a pass energy of 20 eV. UPS spectra were obtained with a pass energy of 5 eV using He II radiation (hν = 40.8 eV) while the work function data was calculated from the He I UPS spectra (hν = 21.2 eV) by measuring the gap between the Fermi edge and the secondary electron edge.

3 Results and discussion

We previously reported C_2H_4 adsorption and surface reaction on Co(0001) at 130 K [18, 21] and thus herein reported C_2H_4 adsorption and surface reaction on Co(0001) at different temperatures. Figure 1 shows TDS spectra of C_2H_4 and H_2 following saturating C_2H_4 exposure on Co(0001) at different temperatures. At 130 K, molecular desorption peaks of C_2H_4 appeared up to around 200 K, meanwhile, two H_2 desorption peaks emerged at around 327 and 421 K, arising from the recombination of H adatoms and the dehydrogenation of molecularly-adsorbed C_2H_2 species (C_2H_2(a)) [18, 21], respectively. As the exposure temperature increased to 300 K, C_2H_4 desorption traces disappeared while only a broad H_2 desorption peak arising from the dehydrogenation of adsorbed C_2H_2(a) emerged at around 405 K. When exposed at 400 K, only a small H_2 desorption peak at around 500 K could be observed.

C 1s XPS spectra of saturating C_2H_4 exposure on Co(0001) at different temperatures on Co(0001) followed by heating to 630 K were shown in Fig. 2. Exposed at 130 K, two C 1s features with the binding energy at 283.6 and 284.4 eV, which could be assigned to adsorbed C_2H_2(a) and molecularly-adsorbed C_2H_4 species (C_2H_4(a)) on Co(0001) [18, 21], respectively. With an increasing of exposure temperature to 300 K, the C 1s feature of adsorbed C_2H_2(a) species at 283.6 eV dominated in the C 1s spectrum. As the exposure temperature further increased to 400 K, the C 1s feature of adsorbed C_2H_2(a) species disappeared, while two C1s features with the binding energy at 283.2 and 284.5 eV emerged and could be assigned to C_2 clusters and graphitic carbon [22], respectively. Exposed at 500 K, the C 1s spectrum was dominated by the C_1 adatoms with the

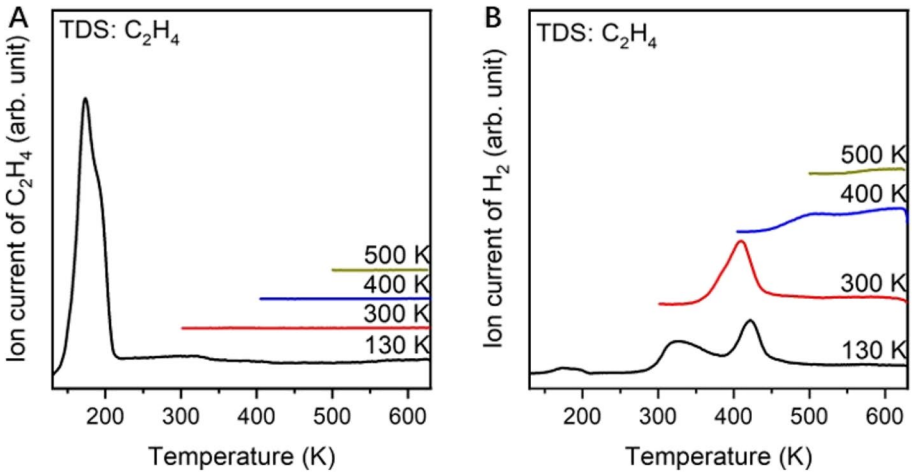

Fig. 1 **A** C_2H_4 and **B** H_2 TDS spectra following saturating C_2H_4 exposure on Co(0001) at indicated temperatures

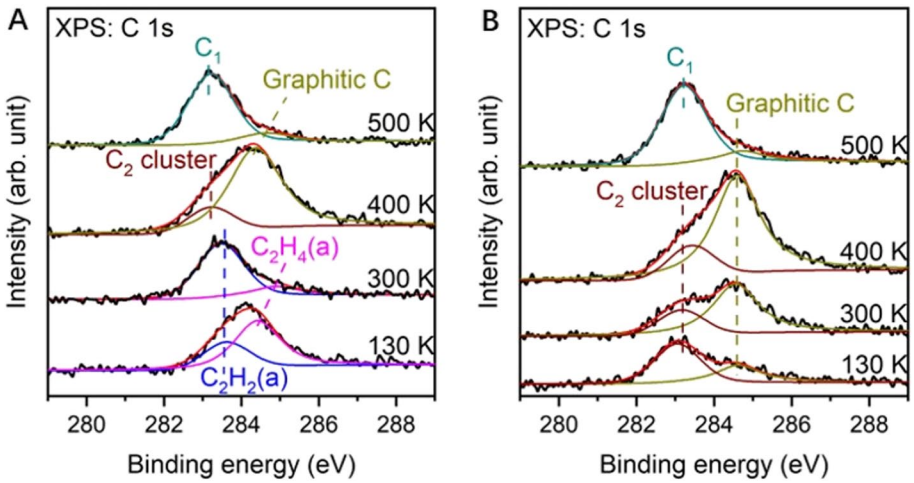

Fig. 2 C 1s XPS spectra of C_2H_4 exposure on Co(0001) at indicated temperatures (**A**) and then followed by subsequent heating to 630 K (**B**)

binding energy at 283.0 eV [22]. Upon subsequent heating to 630 K, the C 1s spectrum of the C_2H_4/Co(0001) surface exposed at 130 K weakened with the disappearance of C_2H_4(a) and C_2H_2(a) features and the emergence of C_2 clusters and graphitic carbon features; the intensity of C 1s spectrum of the C_2H_4/Co(0001) surface exposed at 300 K remained with the disappearance of C_2H_2(a) features and the emergence of C_2 clusters and graphitic carbon features; the C 1s spectra of the C_2H_4/Co(0001) surface exposed at 400 and 500 K did not vary much.

Corresponding He II UPS spectra of saturating C_2H_4 exposure on Co(0001) at different temperatures on Co(0001) and then followed by heating to 630 K were shown in Fig. 3. Exposed at 130 K, four peaks at 6.5, 8.2, 9.3, 13.0 eV below E_F respectively arising from the $1b_{2g}$, $3a_g$, $1b3_u$ and $2a_u$ orbitals of adsorbed C_2H_4(a) species and three peaks at 5.4, 8.9 and 11.3 eV below E_F respectively arising from the 1π, $3\sigma_g$ and $2\sigma_u$ orbitals of adsorbed C_2H_2(a) species [31] appeared in the UPS spectrum. Exposed at 300 K, the features of adsorbed C_2H_2(a) species dominated in the UPS spectrum. Exposed at 400 K, a major broad peak at around 8.7 eV and another small peak at 5.4 eV below E_F appeared, which could be assigned to the orbitals from graphitic carbon and C_2 clusters [18], respectively. Exposed at 500 K, only a peak at around 4.8 eV below E_F was observed, arising from the orbital of C_1 adatoms [18]. Upon subsequent heating to 630 K, the features of C_2 clusters, graphitic carbon, and C_1 adatoms dominated in the UPS spectra of the C_2H_4/Co(0001) surfaces exposed at 130, 300 and 400, and 500 K, respectively. These UPS results were consistent with the above XPS results. It is noteworthy that the

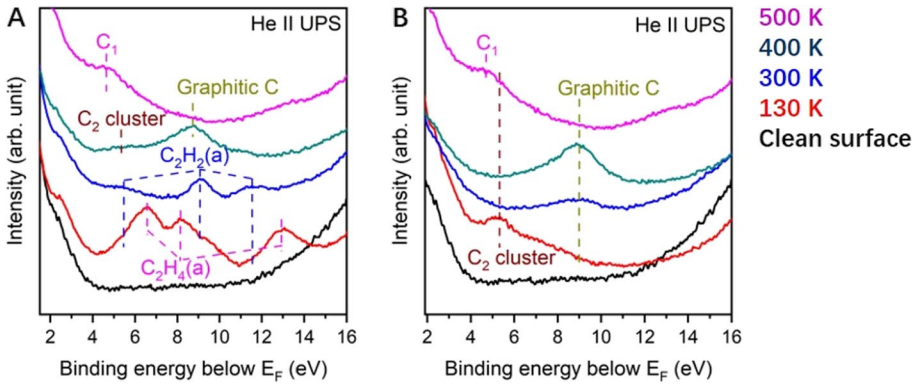

Fig. 3 He II UPS spectra of C_2H_4 exposure on Co(0001) at indicated temperatures (**A**) and then followed by subsequent heating to 630 K (**B**)

feature of adsorbed H atoms resulting from C_2H_4 dissociation should appear in the UPS spectra of C_2H_4 adsorption at 130 and 300 K but not at 400 and 500 K.

The above TDS, XPS and UPS results demonstrated temperature-dependent adsorption and surface reactions of C_2H_4 on Co(0001). C_2H_4 majorly adsorbed molecularly and minorly dissociated into C_2H_2(a) at 130 K. Upon heating, C_2H_4(a) desorbed from the surface before 300 K and C_2H_2(a) further dehydrogenated before 450 K to form C_2 clusters. C_2H_4 dissociated into C_2H_2(a) at 300 K, which, upon heating, dehydrogenated before 450 K to form dominant graphitic carbon. C_2H_4 dissociated directly into dominant graphitic carbon at 400 K while C_1 adatoms at 500 K. These observations indicated that surface reactions of C_2H_2(a) on Co(0001) should depend on the coverage and temperature.

C_2H_2 adsorption on Co(0001) at 130 K was studied by TDS. Only H_2 desorption traces were observed (Fig. 4) but no C_2H_2 desorption traces could be observed. In addition to a recombinative H_2 desorption peak of H adatoms resulting from residual H_2 dissociation at around 380 K, an exposure of 0.01 L C_2H_2 gave another H_2 desorption peak at around 416 K (denoted as α), which could be assigned to the dehydrogenation of adsorbed C_2H_2(a) species. With an increase of C_2H_2 exposure to 0.1 L, the α peak obviously increased, and two minor peaks emerged at around 362 (denoted as β) and 395 K (denoted as γ), corresponding to new C_2H_2(a) dehydrogenation reactions. With the further increase of C_2H_2 exposure up to 10 L, both the β and γ peaks grew while the α peak did not vary much; meanwhile, the β peak shifted to lower temperatures, implying that the corresponding surface reaction kinetics should be larger than the first-order, but the γ peak did not shift, suggesting a first-order desorption kinetics.

C 1s XPS spectra of various exposures of C_2H_2 on Co(0001) at 130 K (Fig. 5A) all showed a single peak at

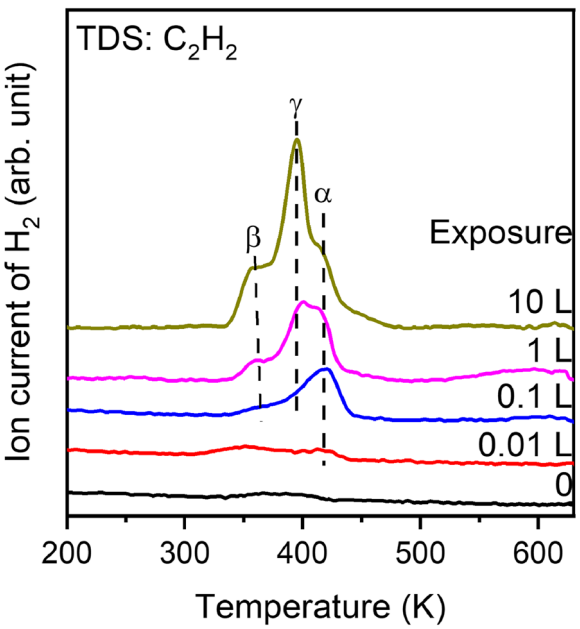

Fig. 4 H_2 TDS spectra following indicated C_2H_2 exposures on Co(0001) at 130 K

283.6 eV arising from adsorbed C_2H_2(a) species. Thus, C_2H_2 exclusively adsorbed on Co(0001) molecularly at 130 K at any coverage. The annealing processes of Co(0001) exposed to 0.1 L and 10 L C_2H_2 at 130 K were studied using XPS and He II UPS. As shown in Fig. 5B, the C 1s feature of C_2H_2(a) following 0.1 L C_2H_2 exposure at 130 K did not change much upon subsequent annealing processes except that the binding energy slightly shifted to 283.5 eV above 400 K, suggesting that C_2H_2(a) exclusively decomposed to produce the H_2 dominantly at around 416 K (the α H_2 desorption peak) and form C_2 clusters with a similar C 1s binding energy to C_2H_2(a). For an exposure of 10 L C_2H_2 (Fig. 5C 1 and 2), the C

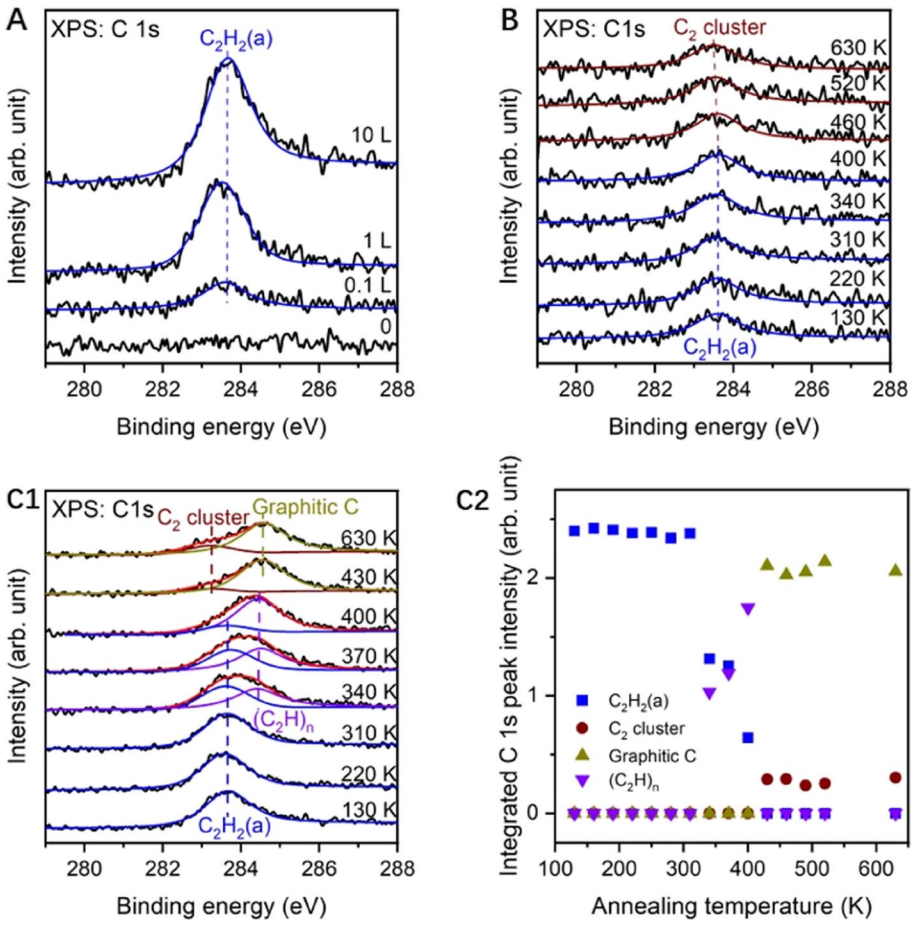

Fig. 5 C 1s XPS spectra of **A** various exposures of C_2H_2 exposure on Co(0001) at 130 K, **B** 0.1 L C_2H_2 exposure on Co(0001) at 130 K followed by annealing at indicated temperatures and (**C1**) C 1s XPS spectra of 10 L C_2H_2 exposure on Co(0001) at 130 K followed by annealing at indicated temperatures, and (**C2**) derived evolutions of various surface species as a function of annealing temperature

1s feature of C_2H_2(a) remained stable up to 310 K and greatly weakened at 340 K, meanwhile, another C 1s feature at 284.4 eV emerged. This new C 1s feature grew and shifted to at 284.5 eV at the expense of the C 1s feature of C_2H_2(a) slightly at 370 K and greatly at 400 K. The C 1s feature of C_2H_2(a) disappeared at 430 K, while a major C 1s peak at 284.6 eV and a minor C 1s peak at 283.3 eV were present on the surface, corresponding to the graphitic carbon and C_2 clusters, respectively. The C 1s XPS spectra remained unchanged upon annealing at higher temperatures up to 630 K. During the annealing processes, the total intensity of C 1s XPS spectrum did not decrease, suggesting that all C_2H_2(a) species underwent dehydrogenation reactions to major graphitic carbon and minor C_2 clusters. In combination with corresponding H_2 TDS spectrum, the major C_2H_2(a) underwent a two-step dehydrogenation process between 340–370 K and 370–430 K to produce the β and γ H_2 desorption peaks, respectively, and the graphitic carbon, while the minor C_2H_2(a) underwent a one-step dehydrogenation process between 400 and 430 K to produce the α H_2 desorption peak and the C_2 clusters. It could be thus inferred that a stable surface intermediate with the C 1s binding energy at around 284.5 eV should exist during the two-step dehydrogenation of C_2H_2(a) into the graphitic carbon.

Figure 6A shows the He II UPS spectra of the annealing processes of Co(0001) exposed to 0.1 L C_2H_2 at 130 K. Adsorbed C_2H_2(a) on Co(0001) showed three features at 5.4, 8.7 and 11.2 eV below E_F arising from its 1π, $3\sigma_g$ and $2\sigma_u$ orbitals, respectively. These features did not change up to 400 K, then the $2\sigma_u$ peak at 11.2 eV disappeared and the $3\sigma_g$ peak at 8.7 eV weakened upon annealing at 430 K, while the 1π peak at 5.4 eV remained unchanged. This indicated the occurrence of C_2H_2(a) dehydrogenation with the carbon–carbon preserved. Upon annealing at 630 K, only a broad peak at 5.4 eV arising from the C_2 clusters could be observed. These UPS results were consistent with the above XPS results that C_2H_2(a) at low

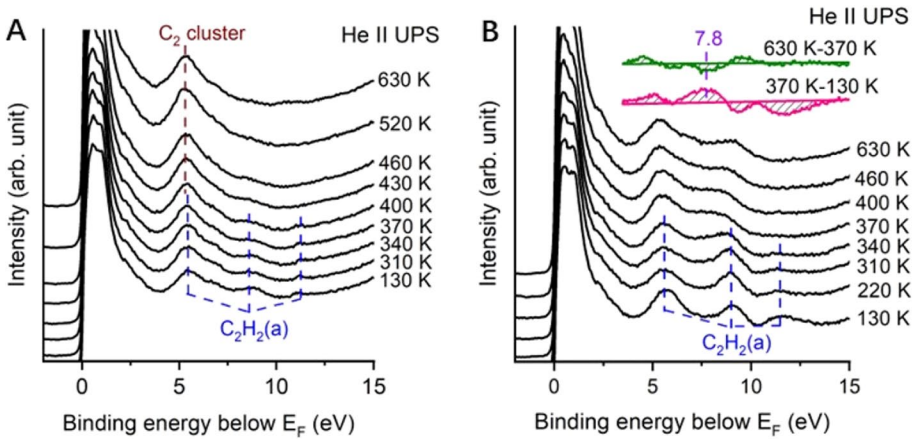

Fig. 6 He II UPS spectra of **A** 0.1 L and **B** 10 L C_2H_2 exposure on Co(0001) at 130 K followed by annealing at indicated temperatures

coverages dehydrogenated into C_2 clusters. Figure 6B shows the He II UPS spectra of the annealing processes of Co(0001) exposed to 10 L C_2H_2 at 130 K. The C_2H_2(a) features remained unchanged upon annealing at 310 K, and then weakened at 340 K and almost disappeared at 370 K. The difference spectrum between the UPS spectra at 370 and 130 K clearly demonstrated an emergence of a new peak at 7.8 eV below E_F at the expense of the C_2H_2(a) features. It was reported that the σ_{CH} bond orbital of adsorbed benzene on Co(0001) film at 300 K located at 7.9 eV below E_F [43]. We then assigned the new feature at 7.8 eV to the σ_{CH} bond in alkyl fragments with carbon ring structures. The difference spectrum between the UPS spectra at 630 and 370 K showed the disappearance of the peak at 7.8 eV, and two features at 9.2 and 5.6 eV below E_F remained in the UPS spectrum annealed at 630 K, which could be assigned to graphitic carbon and C_2 clusters. These UPS results, together with the above XPS and TDS results, suggested the alkyl fragments with carbon ring structures as the surface intermediates for C_2H_2(a) dehydrocyclization into graphitic carbon on Co(0001). It could also be seen that a high C_2H_2(a) coverage suppressed the reaction pathway of C_2H_2(a) dehydrogenation into C_2 clusters due to the limited available vacant surface sites but facilitated the reaction pathway of C_2H_2(a) dehydrocyclization into graphitic carbon.

In order to determine the average C:H stoichiometric of the alkyl fragment intermediates, we compared the H_2 TDS spectra and C 1s XPS spectra of 10 L C_2H_2 exposures on Co(0001) at 130 and 370 K (Fig. 7). Exposed at 370 K, a single H_2 desorption peak at around 450 K and a single C 1s feature at around 284.4 eV appeared in the H_2 TDS spectrum and C1s XPS spectrum, respectively. The C_2H_2(a) dehydrocyclization into the alkyl fragment intermediates with carbon ring structures mainly occurred before 370 K

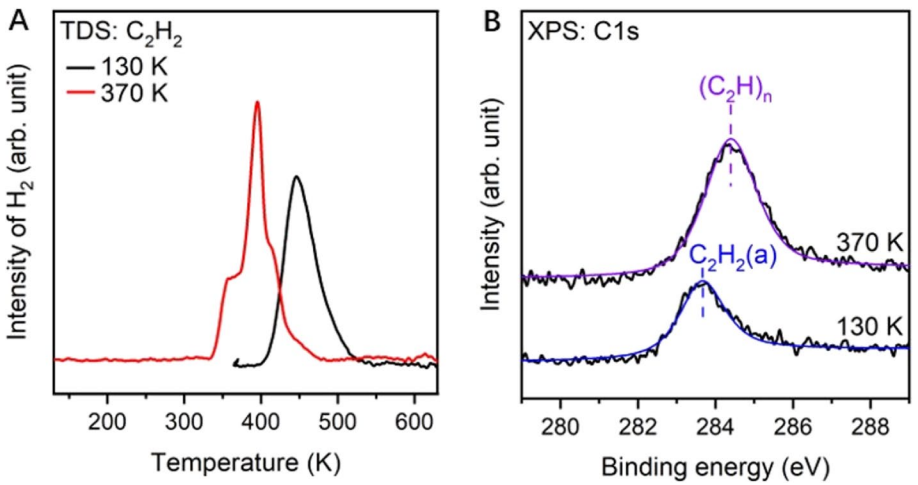

Fig. 7 **A** H_2 TDS spectra and **B** C 1s XPS spectra of 10 L C_2H_2 exposure on Co(0001) at 130 and 370 K

while the subsequent dehydrogenation of alkyl fragment intermediates into graphitic carbon mainly occurred after 370 K, thus the surface species following C_2H_2 exposure at 370 K were dominantly the alkyl fragment intermediates with carbon ring structures. It was found that the C 1s peak intensity/H_2 desorption peak area ratio for 10 L C_2H_2 exposure at 370 K was around half of that for 10 L C_2H_2 exposure at 130 K. Since 10 L C_2H_2 exposure at 130 K exclusively gave C_2H_2(a) with a C:H atomic ratio of 1, the average C:H atomic ratio of the alkyl fragment intermediates was around 0.5. Thus, the alkyl fragment intermediates could be $(C_2H)_n$ species with carbon ring structures. It should be noted that the $(C_2H)_n$ intermediates with carbon ring structures could be with different sizes.

Therefore, similar to C_2H_4, C_2H_2 exhibited temperature-dependent adsorption and surface reactions on Co(0001). C_2H_2 molecularly adsorbed at 130 K. The resulting C_2H_2(a) species at low coverages remained stable up to 400 K and then exclusively dehydrogenated into C_2 clusters, while the resulting C_2H_2(a) species at high coverages remained stable up to 310 K and then majorly dehydrocyclizated into $(C_2H)_n$ intermediates with ring structures at 340 K which further dehydrogenated into graphitic carbon, and minorly dehydrogenated into C_2 clusters. Exposed at 370 K, C_2H_2 dehydrocyclizated into $(C_2H)_n$ intermediates with ring structures.

4 Conclusions

In summary, we have successfully demonstrated temperature and coverage dependent adsorption and surface reactions of C_2H_2 and C_2H_4 on Co(0001). C_2H_4 majorly adsorbed molecularly and minorly dissociated into C_2H_2(a) at 130 K. Upon heating, C_2H_4(a) desorbed from the surface before 300 K and C_2H_2(a) further dehydrogenated before 450 K to form C_2 clusters. C_2H_4 dissociated into C_2H_2(a) at 300 K, which, upon heating, dehydrogenated before 450 K to form dominant graphitic carbon. C_2H_4 dissociated directly into dominant graphitic carbon at 400 K while C_1 adatoms at 500 K. C_2H_2 molecularly adsorbed at 130 K but exclusively dehydrogenated upon heating. The resulting C_2H_2(a) species at low coverages remained stable up to 400 K and then exclusively dehydrogenated into C_2 clusters, while the resulting C_2H_2(a) species at high coverages remained stable up to 310 K and then majorly dehydrocyclizated into $(C_2H)_n$ intermediates with ring structures at 340 K which further dehydrogenated into graphitic carbon, and minorly dehydrogenated into C_2 clusters. Exposed at 370 K, C_2H_2 dehydrocyclizated into $(C_2H)_n$ intermediates with ring structures. These results greatly enrich our fundamental understanding of Co-catalyzed F-T synthesis reaction.

Author contributions

WH supervised the study. LX performed all experiments. ZW, HW, JS and ZL assisted with the experiments. All authors analyzed the data. LX and WH prepared the manuscript.

Funding

This work was supported by the National Natural Science Foundation of China (Grant number U1930203).

Declarations

Competing interests

Weixin Huang is a member of the editorial board of this journal. He was not involved in the editorial review or the decision to publish this article. All authors declare that there are no competing interests.

Received: 1 August 2023 Revised: 12 August 2023 Accepted: 15 August 2023
Published online: 27 September 2023

References

1. Freund HJ, Heyde M, Kuhlenbeck H, Nilius N, Risse T, Schmidt T, Shaikhutdinov S, Sterrer M (2020) Chapter model systems in heterogeneous catalysis at the atomic level: a personal view. Sci China Chem 63:426–447
2. Chen S, Xiong F, Huang W (2019) Surface chemistry and catalysis of oxide model catalysts from single crystals to nanocrystals. Surf Sci Rep 74:100471
3. Huang W (2023) Uniform catalytic nanocrystals: from model catalysts to efficient catalysts. Acc Mater Res 4:373–384
4. Adesina AA (1996) Hydrocarbon synthesis via Fischer-Tropsch reaction: travails and triumphs. Appl Catal A-Gen 138:345–367
5. Schulz H (2013) Principles of Fischer-Tropsch synthesis-constraints on essential reactions ruling FT-selectivity. Catal Today 214:140–151
6. Dry ME (2002) The Fischer-Tropsch process: 1950–2000. Catal Today 71:227–241
7. Dry ME (1990) The Fischer-Tropsch process-commercial aspects. Catal Today 6:183–206
8. Zhang Q, Kang J, Wang Y (2010) Development of novel catalysts for Fischer-Tropsch synthesis: tuning the product selectivity. ChemCatChem 2:1030–1058
9. Zhang Q, Cheng K, Kang J, Deng W, Wang Y (2014) Fischer-Tropsch catalysts for the production of hydrocarbon fuels with high selectivity. Chemsuschem 7:1251–1264
10. Schulz H (2003) Major and minor reactions in Fischer-Tropsch synthesis on cobalt catalysts. Top Catal 26:73–85
11. Sarkari M, Fazlollahi F, Atashi H (2012) Fischer Tropsch synthesis: the promoter effects, operating conditions, and reactor synthesis. Int J Chem React Eng 10:1–30
12. Schulz H (1999) Short history and present trends of Fischer-Tropsch synthesis. Appl Catal A: Gen 186:3–12
13. Khodakov AY, Chu W, Fongarland P (2007) Advances in the development of novel cobalt Fischer–Tropsch catalysts for synthesis of long-chain hydrocarbons and clean fuels. Chem Rev 107:1692–1744
14. Zaera F (1995) An organometallic guide to the chemistry of hydrocarbon moieties on transition metal surfaces. Chem Rev 95:2651–2693
15. Xu H, Jin Y, Xu L, Wang Z, Sun G, Chai P, Huang W (2019) Surface chemistry of CH_2I_2 on clean, hydrogen- and carbon monoxide-covered Co(0001) surfaces. J Phys Chem C 123:7740–7748
16. Xu H, Fu C, Zhang Z, Chai P, Wu L, Wang H, Huang W (2020) Role of coadsorbates in shaping the reaction pathways of alkyl fragments on Co surfaces. J Phys Chem C 124:24786–24794
17. Xu L, Ma Y, Zhang Y, Chen B, Wu Z, Jiang Z, Huang W (2010) Water adsorption on a Co (0001) surface. J Phys Chem C 114:17023–17029
18. Xu L, Ma Y, Zhang Y, Chen B, Wu Z, Jiang Z, Huang W (2011) Surface chemistry of C_2H_4, CO, and H_2 on clean and graphite carbon-modified Co (0001) surfaces. J Phys Chem C 115:3416–3424
19. Xu L, Jin Y, Wu Z, Xiong F, Huang W (2017) Self-anticoking of a cobalt surface by subsurface oxygen in the Fischer-Tropsch synthesis. Chem Eur J 23:3262–3266

20. Jin Y, Sun G, Wang Z, Pan H, Xu L, Xu H, Huang W (2017) Elementary surface reactions on Co(0001) under Fischer-Tropsch synthesis conditions. J Phys Chem C 121:21535–21540
21. Xu L, Ma Y, Wu Z, Chen B, Yuan Q, Huang W (2012) A photoemission study of ethylene decomposition on a Co(0001) surface: formation of different types of carbon species. J Phys Chem C 116:4167–4174
22. Xu L, Jin Y, Wu Z, Yuan Q, Jiang Z, Ma Y, Huang W (2013) Transformation of carbon monomers and dimers to graphene islands on Co(0001): thermodynamics and kinetics. J Phys Chem C 117:2952–2958
23. Habermehl-Cwirzen KME, Kauraala K, Lahtinen J (2004) Hydrogen on cobalt: the effects of carbon monoxide and sulphur additives on the D_2/Co(0001) system. J Phys Scr T108:28–32
24. Lahtinen J, Vaari J, Kauraala K (1998) Adsorption and structure dependent desorption of CO on Co(0001). Surf Sci 418:502–510
25. Böller B, Ehrensperger M, Wintterlin J (2015) In situ scanning tunneling microscopy of the dissociation of CO on Co(0001). ACS Catal 5:6802–6806
26. Weststrate CJ, Niemantsverdriet JW (2018) CO as a promoting spectator species of C_xH_y conversions relevant for Fischer-Tropsch chain growth on cobalt: evidence from temperature-programmed reaction and reflection absorption infrared spectroscopy. ACS Catal 8:10826–10835
27. Weststrate CJ, Sharma D, Rodriguez DG, Gleeson MA, Fredriksson HOA, Niemantsverdriet JW (2020) Mechanistic insight into carbon-carbon bond formation on cobalt under simulated Fischer-Tropsch synthesis conditions. Nat Commun 11:750
28. Toomes RL, King DA (1996) The adsorption of CO on Co (10–10). Surf Sci 349:1–18
29. Bridge ME, Comrie CM, Lambert RM (1997) Chemisorption studies on cobalt single crystal surfaces. Surf Sci 67:393–404
30. Tiscione P, Rovida G (1985) Adsorption and decomposition of ethylene and acetylene on cobalt. Surf Sci 154:L255–L260
31. Albert MR, Sneddon LG, Plummer EW (1984) An UPS study of the chemisorption of acetylene and ethylene on Co(0001). Sur Sci 147:127–142
32. Vaari J, Lahtinen J, Hautojärvi P (1997) The adsorption and decomposition of acetylene on clean and K-covered Co(0001). Catal Lett 44:43–49
33. Ramsvik T, Borg A, Venvik HJ, Hansteen F, Kildemo M, Worren T (2002) Acetylene chemisorption and decomposition on the Co(1120) single crystal surface. Surf Sci 499:183–192
34. Ramsvik T, Borg A, Worren T, Kildemo M (2002) Hybridisation and vibrational excitation of C_2H_2 on Co(0001). Surf Sci 511:351–358
35. Liu JX, Su HY, Sun DP, Zhang BY, Li WX (2013) Crystallographic dependence of CO activation on cobalt catalysts: HCP versus FCC. J Am Chem Soc 135:16284–16287
36. Liu Z, Hu P (2002) A new insight into Fischer-Tropsch synthesis. J Am Chem Soc 124:11568–11569
37. Cheng J, Gong X, Hu P, Lok CM, Ellis P, French S (2008) A quantitative determination of reaction mechanisms from density functional theory calculations: Fischer-Tropsch synthesis on flat and stepped cobalt surfaces. J Catal 254:285–295
38. Gong X, Raval R, Hu P (2005) CH_x hydrogenation on Co(0001): a density functional theory study. J Chem Phys 122:024711
39. Cheng J, Hu P, Ellis P, French S, Kelly G, Lok CM (2008) A DFT study of the chain growth probability in Fischer-Tropsch synthesis. J Catal 257:221–228
40. Zhuo M, Borgna A, Saeys M (2013) Effect of the CO coverage on the Fischer-Tropsch synthesis mechanism on cobalt catalysts. J Catal 297:217–226
41. Zhai P, Chen P, Xie J, Liu J, Zhao H, Lin L, Ma D (2017) Carbon induced selective regulation of cobalt-based Fischer-tropsch catalysts by ethylene treatment. Faraday Discuss 197:207–224
42. Yao Z, Guo C, Mao Y, Hu P (2019) Quantitative determination of C-C coupling mechanisms and detailed analyses on the activity and selectivity for Fischer-Tropsch synthesis on Co (0001): microkinetic modeling with coverage effects. ACS Catal 9:5957–5973
43. Getzlaff M, Bansmann J, Schönhense G (1995) The electronic structure of benzene adsorbed on thin Fe(110) and Co(0001) films. Surf Sci 323:118–128

Publisher's Note